

Three-dimensional cultured tissue constructs that imitate human living tissue organization for analysis of tumor cell invasion

Soichi Iwai,^{1*} Satoko Kishimoto,^{1*} Yuto Amano,² Akihiro Nishiguchi,² Michiya Matsusaki,^{2,3} Akinori Takeshita,¹ Mitsuru Akashi^{2,4}

¹Department of Oral and Maxillofacial Surgery II, Graduate School of Dentistry, Osaka University, 1-8, Yamada-oka, Suita, Osaka 565-0871, Japan

²Department of Applied Chemistry, Graduate School of Engineering, Osaka University, 2-1, Yamada-oka, Suita, Osaka 565-0871, Japan

³PRESTO, Japan Science and Technology Agency (JST), 4-1-8 Honcho Kawaguchi, Saitama, Japan

⁴Graduate School of Frontier Biosciences, Osaka University, 1-3, Yamada-oka, Suita, Osaka 565-0871, Japan

Received 22 September 2017; revised 9 December 2017; accepted 21 December 2017

Published online 5 December 2018 in Wiley Online Library (wileyonlinelibrary.com). DOI: 10.1002/jbm.a.36319

Abstract: Preventing cancer metastasis requires a thorough understanding of cancer cell invasion. These phenomena occur in human 3-D living tissues. To this end, we developed a human cell-based three-dimensional (3-D) cultured tissue constructs that imitate in vivo human tissue organization. We investigated whether our 3-D cell culture system can be used to analyze the invasion of human oral squamous cell carcinoma (OSCC) cells. The 3-D tissue structure consisted of five layers of normal human dermal fibroblasts along with human dermal lymphatic endothelial cell tubes and was generated by the cell accumulation technique and layer-by-layer assembly using fibronectin and gelatin. OSCC cells with different lymph metastatic capacity were inoculated on the 3-D tissues and their invasion through the 3-D tissue structure was observed. Conventional methods of analyzing cell

migration and invasion, that is, 2-D culture-based transwell and Matrigel assays were also used for comparison. The results using the 3-D cultured tissue constructs were comparable to those obtained using conventional assays; moreover, use of the 3-D system enabled visualization of differential invasion capacities of cancer cells. These results indicate that our 3-D cultured tissue constructs can be a useful tool for analysis of cancer cell invasion in a setting that reflects the in vivo tissue organization. © 2018 The Authors. *Journal Of Biomedical Materials Research Part A* Published By Wiley Periodicals, Inc. J. Biomed. Mater. Res. Part A: 107A: 292–300, 2019.

Key Words: three-dimensional (3D) cultured tissue constructs, human oral epithelial tissue, tissue engineering, tumor cell invasion, oral squamous cell carcinoma (OSCC) cells

How to cite this article: Iwai S, Kishimoto S, Amano Y, Nishiguchi A, Matsusaki M, Takeshita A, Akashi M. 2019. Three-dimensional cultured tissue constructs that imitate human living tissue organization for analysis of tumor cell invasion. *J. Biomed. Mater. Res. Part A* 2019;107A:292–300.

INTRODUCTION

Understanding the mechanisms of cancer cell migration and invasion is essential for controlling local invasion or lymphogenous and hematogenous metastasis. Importantly, these phenomena occur in human 3-D living tissues.

In vivo experimental transplantation in animals is typically used, but is associated with some problems. For example, a heterologous graft may provide results different from the human phenomena, chronological observation is difficult, and animal experiments have been restricted in recent years. In contrast, in vitro experiments with conventional analysis of migration and invasion ability based on 2-D culture methods are also typically used to analyze these processes.

For instance, wound healing and transwell assays are used to evaluate cell migration, whereas the Matrigel chamber assay is used to assess cell invasion. However, these assays may not reflect actual events that occur in living tissues. To this end, we developed a 3-D cultured tissue system using the layer-by-layer (LbL) approach^{1,2} consisting of a multilayered tissue with normal human dermal fibroblasts (NHDFs) and human dermal lymphatic endothelial cells (HDLECs), which was similar to human subcutaneous tissue [Fig. 1(A)].

The oral mucosa and skin are composed of stratified squamous epithelium. Almost all oral cancers are squamous cell carcinomas, which are derived from stratified squamous epithelial cells. Oral cancer cells that occur in the epidermis

Additional Supporting Information may be found in the online version of this article.

*These authors contributed equally to this work.

Correspondence to: Soichi Iwai; e-mail: s-iwai@dent.osakau.ac.jp

Contract grant sponsor: Grants-in-Aid for Scientific Research (KAKENHI) from the Japan Society for the Promotion of Science; contract grant number: 17K11872

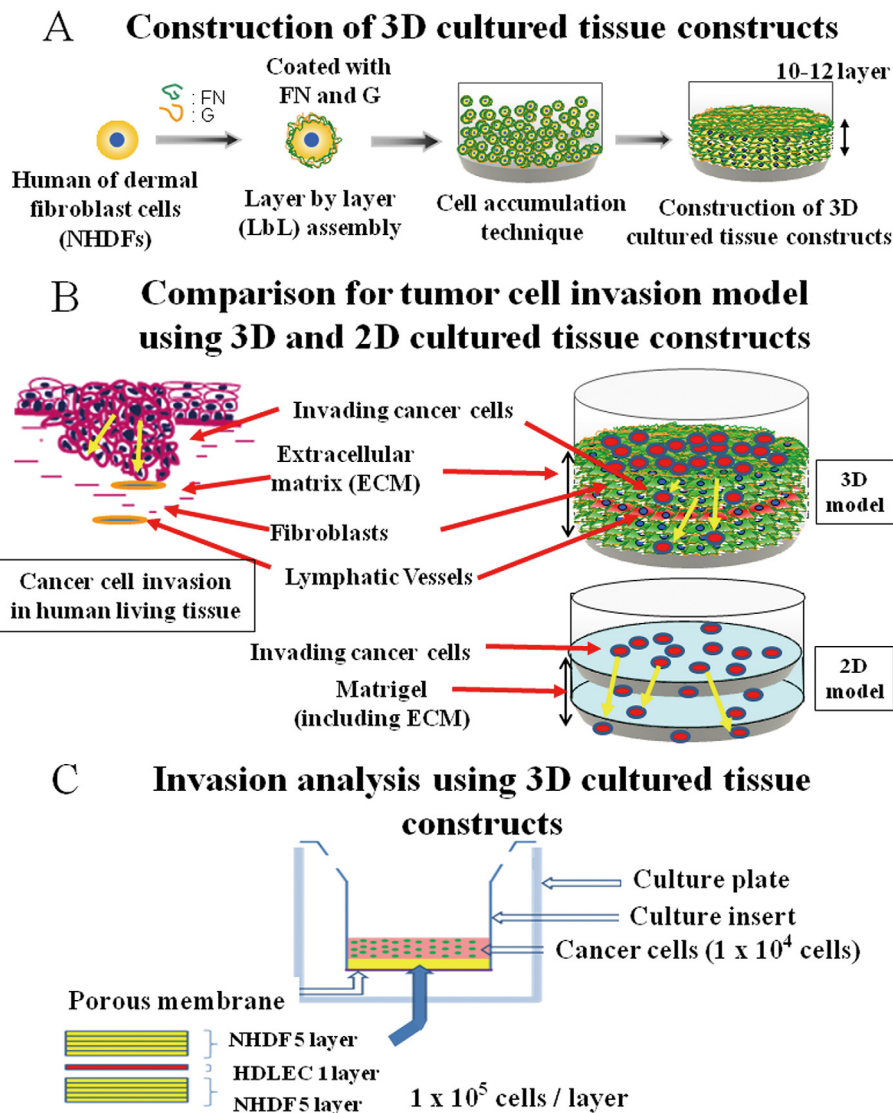


FIGURE 1. A: Construction of 3-D cultured tissue constructs. NHDFs are coated with fibronectin and gelatin via layer-by-layer (LbL) assembly, and a 3-D cultured tissue is constructed using the cell accumulation technique. In this manner, we developed a 3-D cultured tissue construct that imitates the human living tissue organization. **B:** Schematic illustration for comparison for tumor cell invasion model using 3-D and 2-D cultured tissue constructs. Our 3-D invasion model better resembles the environment of the living body tissue than a 2-D invasion model. Our purpose was to compare the ability of the 3-D cultured tissue constructs to assess tumor cell migration and invasion ability to that of conventional 2-D cell culture methods. **C:** Schematic illustration of the invasion assay based on 3-D cultured tissue constructs. The tissue consisted of five layers of NHDFs, one layer of HDLECs, and five layers of NHDFs. Tumor cell suspensions were adjusted to a concentration of 1×10^4 cells per 300 μL of medium and cultured on 3-D tissues for 5 days. The invasion of SAS-Venus cells and SAS-LM8 cancer cells through the structure was then observed.

(the outer layer of epithelium) destroy the basement membrane and invade the dermis (the inner layer of epithelium), in which fibroblasts, lymphatic vessels, blood vessels, and extracellular matrix (ECM) including collagen fibers exist. For investigation of tumor cell invasion, it has been necessary to develop 3-D tissue constructs imitating human living tissues such as the human epithelium.

Recently, several studies of tumor cell invasion in 3-D models have been reported. For example, breast cancer cell invasion was quantified using a 3-D model.³ A cancer cell spheroid assay was used to assess invasion in a 3-D setting.⁴ Cell spheroids have been employed as 3-D culture models, especially 3-D cancer spheroids for modeling of cancer cell

metastasis. Although interesting 3-D-co-culture spheroids have been reported for the investigation of tumor invasion, the reconstruction of the delicate and precise 3-D location of multiple types of cells has not been achieved yet due to cell heterogeneity, the lack of control of cell number and location, and necrosis inside the spheroids because of insufficient nutrient supply. Recently, several bottom-up approaches such as a cell sheet⁵⁻⁷ and cell-containing gel layer⁸ have been reported for the construction of multilayered tissues. These methods are intriguing, but have limitations due to the complicated manipulation of fragile cell sheets.

We previously developed a simple bottom-up approach by preparing nanometer-sized ECM films on cell surfaces⁹⁻¹¹

using fibronectin-gelatin (FN-G) films with a thickness of <10 nm, prepared by layer-by-layer (LbL) assembly.¹²⁻¹⁴ These films promoted cell-cell interactions similar to natural ECM. This technique is simple but can be used to develop multilayered constructs while controlling the cellular type and location. However, the fabrication of multilayer tissues is limited due to the time required for stable cell adhesion.

Therefore, we have developed a simple bottom-up approach, called the cell accumulation technique.¹ Our simple approach through nano-ECM film fabrication easily provides approximately 3-D tissue constructs with 8-10 layers after only one day of incubation. Using our simple and rapid cell-accumulation technique, the layer number, cell type, and location were successfully controlled by altering the seeding cell number and order.

We previously reported that SAS-Venus and SAS-LM8, which are highly metastatic lymph cells, showed increased migration and invasion in a 2-D cell culture system upon stimulation with Wnt5b.¹⁵⁻¹⁷ In this study, we investigated whether our 3-D cell culture system can be used to analyze the migration and invasion of human oral squamous cell carcinoma (OSCC) cells and compared the results to those obtained using conventional 2-D cell culture methods.

MATERIALS AND METHODS

Cell lines and culture

The SAS cell line was derived from surgical specimens of poorly differentiated SCC obtained from a Japanese woman with a primary tongue lesion.¹⁸ SAS-Venus and SAS-LM8 human SCC cell lines stably overexpressing green fluorescent Venus protein were provided by Professor T. Yoneda, Osaka University Graduate School of Dentistry, Japan. Highly lymph metastatic SAS-LM8 human SCC cells (SAS-LM8 cells) were established from SAS-Venus human SCC cells (SAS-Venus cells) through eight rounds of *in vivo* selection^{15,16} (Supporting Information, Fig. 1). HSC3 cells were derived from poorly differentiated OSCC¹⁹ and provided by Riken BioResource Center, Cell Engineering Division (RCB1975) (Ibaraki, Japan). HSC3-Venus human SCC cells (HSC3-Venus cells) stably overexpressing green fluorescent Venus protein were prepared by the same method as SAS-Venus cells.³ The GFP expression vector, pZGreen1-N1, was obtained from Clontech (CA, USA). For gene transfer, plasmid DNA and the gene transfer reagent FuGENE 6 (Promega, WI, USA) were used in a ratio of 1:3, mixed with MEM without addition of FBS. G-418 (Thermo Fisher Scientific, MA) was added to the medium at a concentration of 500 µg/mL, and cells expressing GFP were selectively cultured. Under visual confirmation of GFP by LED light (Optocode, Tokyo, Japan), colonies expressing GFP were cloned.

NHDFs and HDLECs were obtained from Lonza (Basel, Switzerland) and used at passage 4; the cells were cultured in Dulbecco's modified Eagle medium (DMEM) with 10% fetal bovine serum (FBS) at 37°C in a humidified atmosphere of 5% CO₂.

Cell stimulation with recombinant Wnt5b

Cells were cultured with recombinant human Wnt5b (500 ng/mL) (R&D Systems, Minneapolis, MN, USA) for 48 h at 37°C and then used for experiments.

Cell migration and invasion assays

Cell migration was evaluated with transwell assays using BD BioCoat cell culture inserts (Becton-Dickinson, Franklin Lakes, NJ, USA). Cells were resuspended in serum-free DMEM and added to the upper chamber at a density of 5×10^4 cells/insert. DMEM containing 10% FBS was added to the lower chamber. After incubation at 37°C for 48 h, cells that penetrated through the membrane to the lower side were fixed with 4% paraformaldehyde, and stained by Mayer's hematoxylin (Muto, Tokyo, Japan). To measure cell invasion activity, the same assay was performed using BD BioCoat Matrigel invasion chambers (Becton-Dickinson). Cell migration activity and invasiveness were determined by measuring the area occupied by the cells on the lower side of the filter under a fluorescence microscope in 10 randomly selected fields at 200× magnification and quantified using the public domain ImageJ program.¹⁷ The area occupied by the cells that passed through the membrane was calculated. The measurement was repeated in three specimens.

For the data shown in Figures 2(C) and 3(C), rather than Mayer's hematoxylin (Muto, Tokyo, Japan), the area occupied by the cells on the lower side of filter through the pores was measured under a fluorescence microscope.

Nanofilm coating by LBL filtration

Fibronectin (FN) from human plasma (MW = 4.6×10^5 Da) was purchased from Sigma-Aldrich (St. Louis, MO, USA), and gelatin (G) (MW = 1.0×10^5 Da) was purchased from Wako Pure Chemical Industries (Osaka, Japan). All chemicals were used without purification. For LbL filtration, 2.5 mL of a solution containing 0.2 mg/mL FN and G in 50 mM Tris-HCl (pH = 7.4) were added to three wells of a 6-well plate. NHDFs dissociated with 0.1% trypsin were resuspended in 500 µL of 0.2 mg/mL FN and G/Tris-HCl solution and transferred to a 6-well plate culture insert with a membrane pore size of 0.4 µm (Corning, Inc., Corning, NY, USA). The insert was placed in the well containing the FN and G/Tris-HCl solution and alternately incubated for 1 min in a shaking incubator (SI-300; As One Co., Osaka, Japan) and washed. To collect the coated cells at each step, the insert was transferred to an empty well and shaken horizontally at 1.1 g to filter the cell suspension.²

Construction of 3-D tissues by cell accumulation

Cell surfaces were coated with FN-G nanofilms applied over nine steps, then resuspended at a concentration of 5×10^5 cells per 300 µL of DMEM with 10% FBS and seeded in 24-well cell culture inserts with a semipermeable membrane placed in a 6-well culture plate. Medium (1 mL) was added to each well, followed by incubation for 1 h. An additional 1 mL of medium was added to each well to connect the media on the inner and outer portions of the inserts, followed by incubation at 37°C and 5% CO₂ for 24 h. This

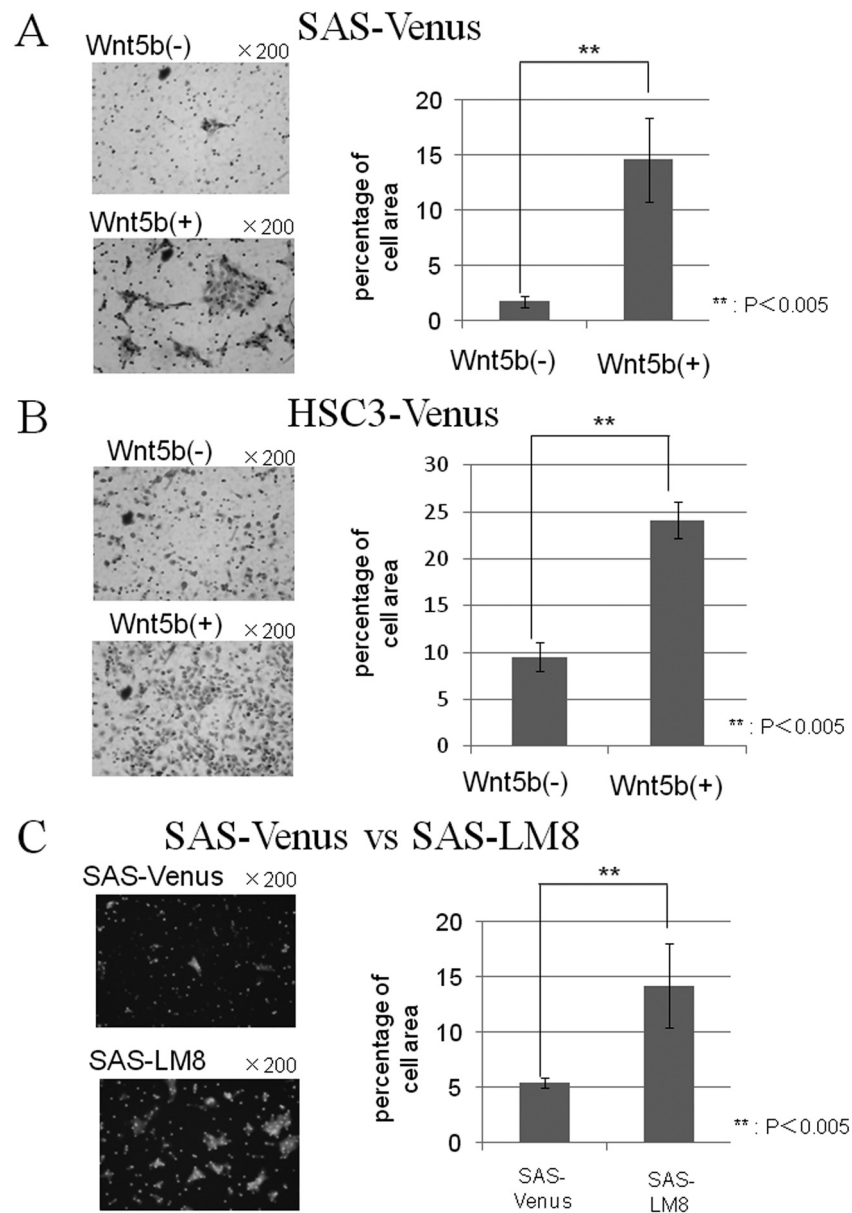


FIGURE 2. Migration assays for SAS-Venus (A) and HSC3-Venus (B) cells stimulated with Wnt5b (500 ng/mL, 48 h). C: Migration assay for SAS-Venus cells relative to SAS-LM8 cells. SAS-Venus, HSC3-Venus, and SAS-LM8 cells stably overexpressing green fluorescent Venus protein. Wnt5b (\pm): recombinant human Wnt5b was added to the culture solution at a concentration of 500 ng/mL and cultured for 48 h at 37°C. The area occupied by the cells on the lower side of the filter was measured under a fluorescence microscope in 10 randomly selected fields at 200 \times magnification and quantified using the public domain software ImageJ. Each column indicates the mean \pm SD of 3 separate experiments. * p < 0.05, ** p < 0.005.

yielded a tissue with five layers of NHDFs. EGM-2 MV (Lonza) was used as the medium for HDLEC cultures and the cells were grown to confluence, dissociated by treatment with 0.1% trypsin, and resuspended in DMEM containing 10% FBS. The cell suspension was adjusted to 1×10^5 cells and inoculated on the 3-D NHDF tissue. After 12 h of culture, NHDFs were coated with FN-G nanofilms following a procedure similar to that described above and seeded in 24-well cell culture inserts with a semipermeable membrane placed in a 6-well cell culture plate. Medium (1 mL) was added to each well. After 1 h of incubation, an additional 1 mL of medium was added to connect the media inside and

outside the inserts, followed by incubation at 37°C and 5% CO₂. After 2 or 3 days of culture, the 3-D tissue comprised five layers of NHDFs, one layer of HDLECs, and five layers of NHDFs [Fig. 1(B)].

Invasion assay using 3-D tissue-cultured constructs

OSCC cells (SAS-Venus and HSC-Venus cells with or without Wnt5b stimulation and SAS-LM8 cells) were resuspended in DMEM containing 10% fetal calf serum (FCS) at 1×10^4 cells/300 μ L, and inoculated on the 3-D tissues and cultured for 5 days at 37°C and 5% CO₂. The migration of cancer cells through the 3-D tissue constructs was observed. Three

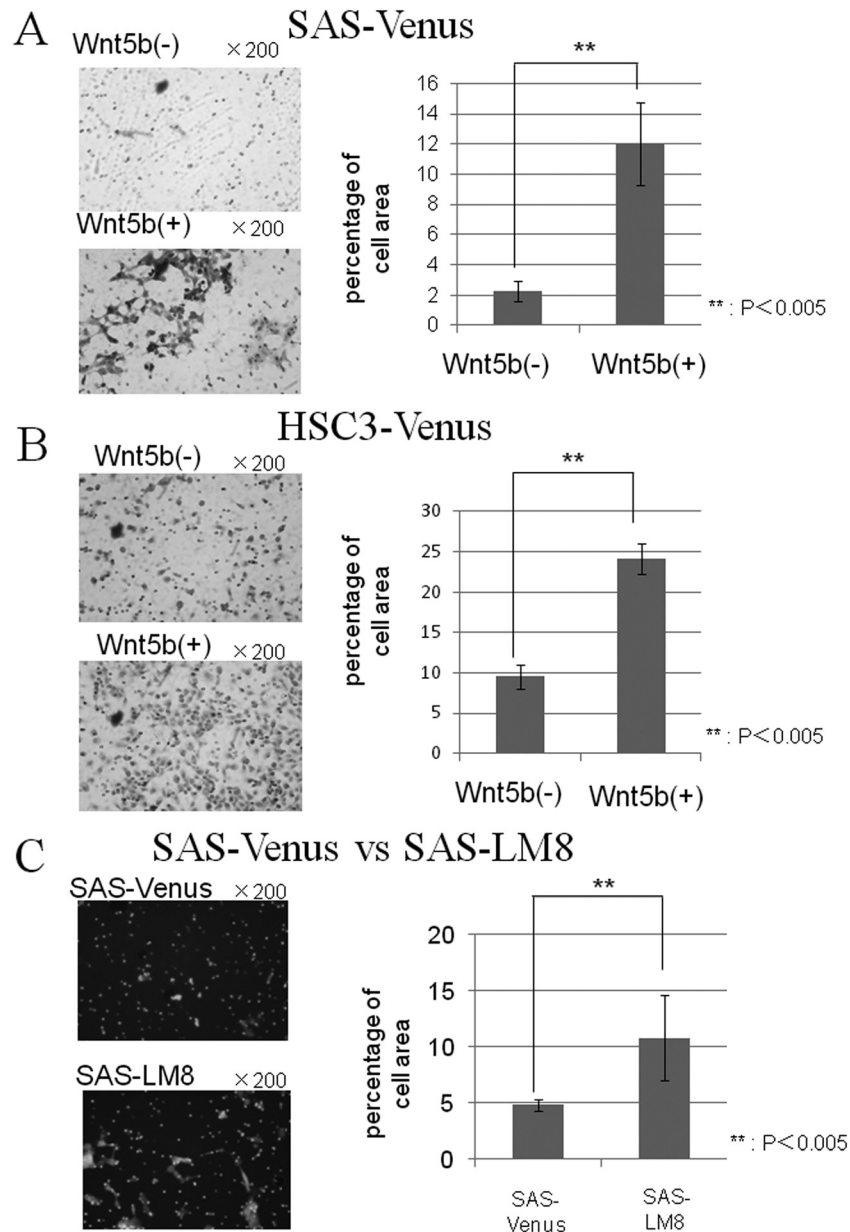


FIGURE 3. Invasion assay using a Matrigel chamber for SAS-Venus (A) and HSC3-Venus (B) cells stimulated with Wnt5b. C: Invasion assay using a Matrigel chamber for SAS-Venus cells relative to SAS-LM8 cells. SAS-Venus, HSC3-Venus, and SAS-LM8 cells stably overexpressing green fluorescent Venus protein. Wnt5b(±): recombinant human Wnt5b was added to the culture solution at a concentration of 500 ng/mL and cultured for 48 h at 37°C. The measurement method was the same as that in Figure 2. * $p < 0.05$, ** $p < 0.005$.

randomly selected views were imaged for each of the three specimens. The number of cells that reached the membrane at the bottom of the 3-D tissue construct, which had a length of ~280 μm in each view, was counted manually. This experiment was repeated twice independently.

Histology and immunohistochemical analysis

Paraffin-embedded 3-D tissues were sectioned at a thickness of 6 μm ; the sections were stained with hematoxylin and eosin. For immunohistochemistry, sections were deparaffinized, and incubated for 5 min at 20°C with proteinase K (Dako, Glostrup, Denmark) diluted 1:1000 in phosphate-buffered saline [PBS (-)] followed by 3%

hydrogen peroxide. After washing, sections were incubated in 1% bovine serum albumin for at least 20 min at room temperature. A mouse monoclonal antibody against human cytokeratin (CK) (Dako) diluted 1:500 was added overnight at 4°C, followed by incubation for 30 min at room temperature with horseradish peroxidase-conjugated antimouse secondary antibody (Dako). After washing with PBS (-), staining with diaminobenzidine (Dako), and nuclear staining with Mayer's hematoxylin for 30 s, sections were washed and imaged under a light microscope (400 \times magnification) with an AxioCamERc5s digital camera (Carl Zeiss, Oberkochen, Germany). Three randomly selected views were imaged for each of the three

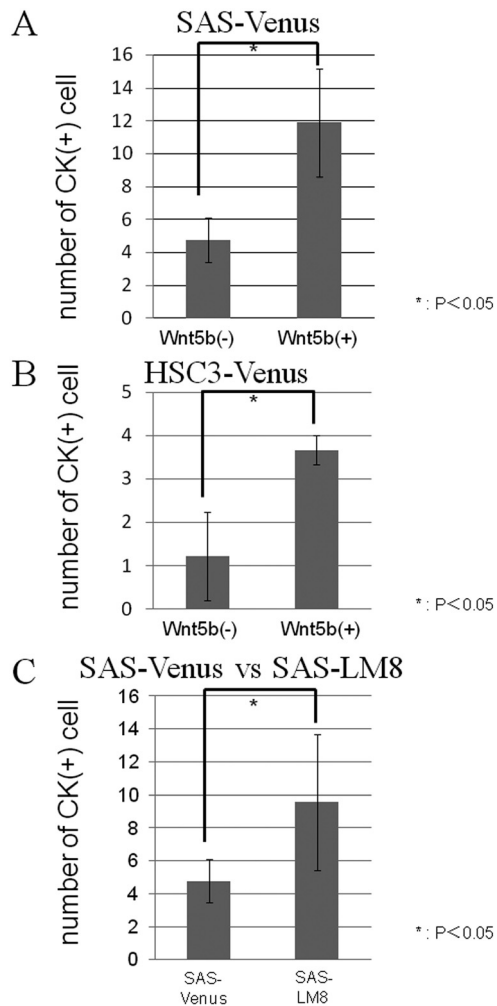


FIGURE 4. Invasion assay using 3-D tissue constructs. The number of cells that reached the membrane at the bottom of the 3-D tissue was counted in each view manually. SAS (A) and HSC-3 (B) cells stimulated by Wnt5b. C: SAS-LM8 cells relative to SAS-Venus cells. Three randomly selected views were imaged for each of the three specimens. * $p \leq 0.05$.

specimens. The average of number of CK-positive cells that reached the membrane at the bottom of the 3-D tissue was determined.

Statistical analysis

Student's *t* test was used to compare group means. $p < 0.05$ was considered statistically significant.

RESULTS

In the transwell migration assay, we measured the area occupied by cells on the lower side of the filter after their migration through the pores for 48 h. The area was 8.1-fold higher for SAS-Venus cells stimulated with Wnt5b as compared to that for unstimulated cells (14.6% vs. 1.8%; $p \leq 0.005$) [Fig. 2(A)]. Similarly, the area was 2.4-fold higher for Wnt5b-stimulated HSC-3 Venus cells than that for unstimulated cells (9.8 vs. 23.8%; $p \leq 0.005$) [Fig. 2(B)].

Similar trends were observed in the Matrigel invasion assay; the cell-covered areas of Wnt5b stimulated SAS- and HSC3-Venus cells were 5.2- and 2.5-fold higher, respectively, than that of unstimulated cells (12.0% vs. 2.3% and 24.1% vs. 9.5%, respectively; $p \leq 0.005$) [Fig. 3(A,B)].

In the transwell migration assay, SAS-LM8 cells covered an area that was 2.7-fold larger than the area occupied by SAS-Venus cells (5.4% vs. 14.6%; $p \leq 0.005$) [Fig. 2(C)]. In the Matrigel invasion assay, the SAS-LM8 cell-covered area was 2.2-fold higher than the SAS-Venus cell-covered areas (4.9% vs. 10.9%; $p \leq 0.005$) [Fig. 3(C)].

The difference in the migration and invasion activity of SAS-Venus cells in the presence of Wnt5b stimulation (8.1-fold and 5.2-fold, respectively) was larger than that of SAS-Venus and SAS-LM8 cells (2.7-fold and 2.2-fold, respectively). The difference in the migration and invasion activity of SAS-Venus cells in the presence of Wnt5b stimulation (8.1-fold and 5.2-fold, respectively) was larger than that of HSC3-Venus cells (2.4-fold and 2.5-fold, respectively). The same results were obtained when two or more researchers performed these assays independently.

In the invasion analysis, we measured the number of CK-positive cells that reached the lower side of the 3-D culture tissue constructs after passing through the structure. The number of SAS-Venus cells that reached the lower side of the 3-D culture tissue upon stimulation by Wnt5b was 2.7-fold greater than that for cells without Wnt5b stimulation (12% vs. 4.5%, $p < 0.05$) [Fig. 4(A)].

The amount of Wnt5b-stimulated HSC-3 cells that reached the lower side of the 3-D culture tissue was 3-fold higher than that of Wnt5b nonstimulated HSC-Venus cells (3.6% vs. 1.2%; $p < 0.05$) [Fig. 4(B)]. The area covered by SAS-LM8 cells was 2.3-fold larger than the area covered by SAS-Venus cells (9.8% vs. 4.2%; $p < 0.05$) [Fig. 4(C)].

The difference in the invasion activity of SAS-Venus cells in the presence of Wnt5b stimulation (2.7-fold) was somewhat larger than that of SAS-Venus and SAS-LM8 cells (2.3-fold). The difference in the invasion activity of SAS-Venus cells in the presence of Wnt5b stimulation (2.7-fold) was almost the same as that of HSC3-Venus cells in the presence of Wnt5b stimulation (3.0-fold).

Importantly, we clearly observed the invasion of these cancer cells into the 3-D tissue structure [Fig. 5(A,B)]. More SAS-LM8 cells than SAS-Venus cells moved toward and reached the bottom of the structure [Fig. 4(B), arrows]. Moreover, we observed that HDLEC cells formed capillary-like extensions in the 3-D structure [Fig. 5(C), arrows].

Moreover, we visualized the tumor cell invasion in the 3-D tissue constructs using immunofluorescence (Supporting Information, Fig. 3). SAS-Venus cells and SAS-LM8 cells were recognized as GFP Venus-positive (green). HDLECs (human dermal lymphatic endothelial cells) reacted with a mouse monoclonal antibody against human CD31 (Dako Denmark) and Alexa Fluor 546-labeled goat anti-mouse IgG antibody (Invitrogen CA USA) (red). DAPI staining mainly indicated NHDFs (normal human dermal fibroblasts) (blue). We could confirm that HDLECs formed lymphatic capillary networks.

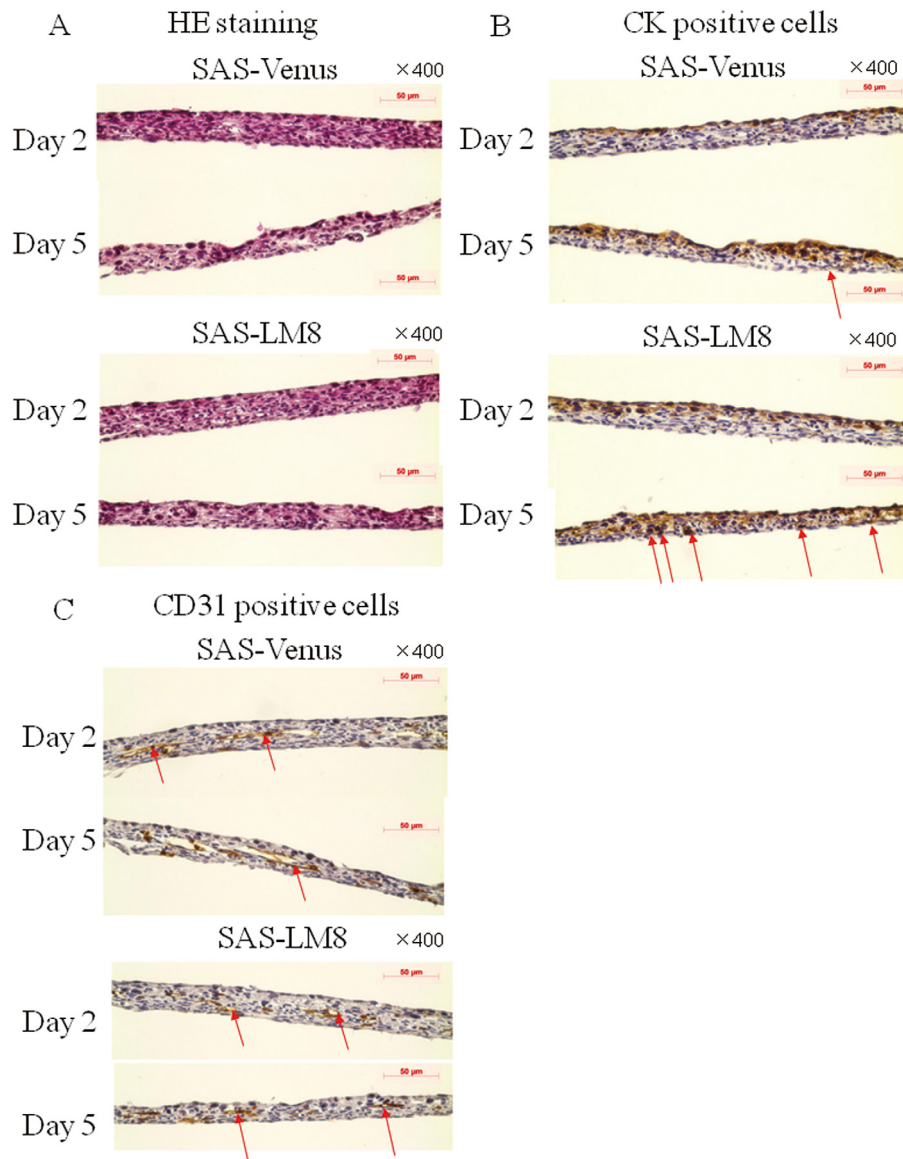


FIGURE 5. A: 3-D Tissue organization, as observed by hematoxylin and eosin staining. **B:** Tumor cells were detected using an anti-CK antibody. Arrows indicate cancer cells that reached the bottom of the 3-D tissue structure. **C:** IHDLECs were detected using an anti-CD31 antibody; the cells formed capillary-like extensions (arrows). Images are shown at 10x magnification.

DISCUSSION

When SCC cells undergo oncogenic transformation within the epithelial tissue, the basement membrane is destroyed and the cells invade the underlying stroma, which consists of fibroblasts, extracellular matrix (ECM), and collagen fibers, among other components.^{20,21} Cancer cells invade blood and lymph vessel endothelial cells and pass through these vessels, resulting in distant or regional lymph node metastasis. These processes are mediated by complex and dynamic interactions involving various cell types and the ECM in the tumor microenvironment.²² For example, surrounding fibroblasts promote tumor progression, motility, and malignancy, and some tumor cells induce angiogenesis and lymphangiogenesis.^{23,24} Therefore, establishing 3-D constructs that imitate the 3-D tumor microenvironments can provide mechanistic insight into the process of tumor invasion.

Recently, 3-D culture systems have been developed that display the features of actual tissue, including cell shape, chemoresistance, hypoxia gradient, and angiogenic capacity, in contrast to 2-D models.^{25–28} However, most of these 3-D tissue constructs, including spheroid culture systems, are heterocellular. In this study, we evaluated whether a 3-D cultured tissue system is more useful for analyzing human OSCC cell migration and invasion than conventional methods based on 2-D cell cultures. Invasion was also increased in the 3-D cultured tissue constructs. Our findings are consistent with those of a previous study reporting that SAS-Venus cell migration and invasion were increased by stimulation with Wnt5b.¹⁷

We investigated and confirmed the proliferative capacity of each cell type or each condition in 2-D conventional cell culture. For example, no difference in proliferative capacity

was observed between SAS-Venus cells and SAS-LM8 cells.¹⁷ Moreover, no difference in proliferative capacity was observed between SAS-Venus Wnt5(-) and SAS-Venus Wnt5(±) cells or between HSC-Venus Wnt5(-) and HSC-Venus Wnt5(±) cells (data not shown).

We showed that SAS-LM8 and SAS-Venus cells undergo cervical lymph node metastasis in a mouse model,¹⁵ with a 2.5-fold higher rate of metastasis for SAS-LM8 cells (Supporting Information, Fig. 1). There was no difference in proliferation between SAS-Venus and HSC3-Venus cells with or without Wnt5b stimulation and SAS-LM8 cells.¹⁷ In the wound healing assay, SAS-LM8 cells occupied a larger area than SAS-Venus cells (98% vs. 62%; $p < 0.05$) (Supporting Information, Fig. 2).

The results in Figure 2 indicate the migration activity, that is, the chemotaxis of tumor cells to FBS as a chemoattractant. The results in Figure 3 indicate the invasion activity, that is, the capacity of tumor cells to dissolve Matrigel using MMPs and then penetrate the Matrigel. The process of tumor cell invasion is affected by many factors. The results in Figure 4 show that the tumor cells migrate through fibroblasts and move by dissolving the stroma in the 3-D space. When analyzing the invasion process of tumor cells, this 3-D tissue construct may be more similar to living body tissue than 2-D cultures.

The results obtained with the 3-D tissue culture system were consistent with those obtained using conventional methods based on 2-D cultures. Importantly, this method enabled visualization of tumor cell invasion through the 3-D cultured structure by immunohistochemistry.

Moreover, our system may enable observation of the process of cancer cell invasion using 3-D constructs of human tissue complete with lymph vessel endothelial cells mimicking stromal tissue. It also enabled estimation of the average distance from a given cancer cell to HDLECs based on immunofluorescence labeling (data not shown). In this manner, the invasion of blood vessels and lymphatic vessels can be analyzed in detail.

Moreover, using our model, it may be possible to analyze time- or area-specific changes in mRNA or protein expression in cancer cells or surrounding tissue. For example, cancer cells invade the stroma and secrete matrix metalloproteinases (MMPs) that destroy the ECM, whereas surrounding fibroblasts promote tumor progression and malignancy.²³ Moreover, some tumor cell types induce angiogenesis and lymphangiogenesis.²⁴ MMPs are involved in tumor growth, differentiation, migration, invasion, and apoptosis.^{29,30} However, it is difficult to identify the MMPs that are secreted from cancer cells during invasion using a 2-D culture system or xenograft models. Our 3-D cultured tissue system would allow observation of the MMPs secreted by cancer cells at different stages of invasion, providing a mechanistic understanding of cell-cell and cell-ECM interactions that could provide a basis for the development of effective drugs to prevent metastasis.

As a future direction, human squamous epithelium tissue constructs could be constructed for drug toxicity testing. We will construct not only lymph endothelial tube networks but

also capillary networks and cultured them with many types of cells, for example, immunocytes, and with blood substitute. These 3-D tissue constructs will replicate the processes of tumor cell invasion, intravasation, tumor angiogenesis, and extravasation. For preclinical anticancer drug assays, 3-D tissue constructs with vascularized structures have the potential to reproduce drug responses individually.

In conclusion, our 3-D cultured tissue constructs allow detailed analysis of cancer cell migration and invasion in an environment that imitates actual human tissue. It is expected that the expression of genes and proteins involved in these processes can be evaluated using this system.

ACKNOWLEDGMENTS

The authors thank Dr Toshiyuki Yoneda (Adjunct and Emeritus Professor, Department of Biochemistry, Graduate School of Dentistry, Osaka University, Japan and Senior Research Professor, Division of Hematology/Oncology, Indiana University School of Medicine, USA) and Dr Kenji Hata (Associate Professor, Department of Biochemistry, Graduate School of Dentistry, Osaka University, Japan) for providing SAS-Venus and SAS-LM8 cells.

They thank Editage (www.editage.jp) for English language editing.

REFERENCES

- Nishiguchi A, Yoshida H, Matsusaki M, Akashi M. Rapid construction of three-dimensional multilayered tissues with endothelial tube networks by cell accumulation technique. *Adv Mater* 2011;23:3506–3510.
- Amano Y, Nishiguchi A, Matsusaki M, Iseoka H, Miyagawa S, Sawa M, Seo M, Yamaguchi T, Akashi M. Development of vascularized iPSC derived 3D-cardiomyocyte tissues by filtration layer-by-layer technique and their application for pharmaceutical assays. *Acta Biomater* 2016;33:110–121.
- Cvetkovic D, Goertzen G-FC, Bhattacharya M. Quantification of breast cancer cell invasiveness using a three-dimensional (3D) model. *J Vis Exp* 2014;88:51341.
- Berens BE, Holy MJ, Riegel TA, Wellstein A. A cancer cell spheroid assay to assess invasion in a 3D setting. *J Vis Exp* 2015;105:53409.
- Kushida A, Yamato M, Konno C, Kikuchi A, Sakurai Y, Okano T. Decrease in culture temperature releases monolayer endothelial cell sheets together with deposited fibronectin matrix from temperature-responsive culture surfaces. *J Biomed Mater Res* 1999;1545:355–362.
- Sasagawa T, Shimizu T, Sekiya S, Haraguchi Y, Yamato M, Sawa Y, Okano T. Design of prevascularized three-dimensional cell-dense tissues using a cell sheet stacking manipulation technology. *Biomaterials* 2010;31:1646–1654.
- Asakawa N, Shimizu T, Tsuda Y, Sekiya S, Sasagawa T, Yamato M, Fukai F, Okano T. Pre-vascularization of in vitro three-dimensional tissues created by cell sheet engineering. *Biomaterials* 2010;31:3903–3909.
- Grossin L, Cortial D, Saulnier B, Felix O, Chassepot A, Decher G, Netter P, Schaaf P, Gillet D, Mainard D, Voegel JC, Benkirane-Jessel N. Step-by-step build-up of biologically active cell-containing stratified films aimed at tissue engineering. *Adv Mater* 2009; 21:650–655.
- Matsusaki M, Kadowaki K, Nakahara M, Akashi M. Fabrication of cellular multilayers with nanometer-sized extracellular matrix films. *Angew Chem Int Ed Engl* 2007;46:4689–4692.
- Matsusaki M, Kadowaki K, Adachi E, Sakura T, Yokoyama U, Ishikawa Y, Akashi M. Morphological and histological evaluations of 3D-layered blood vessel constructs prepared by hierarchical cell manipulation. *J Biomater Sci Polym Ed* 2012;23:63–79.

11. Kadowaki K, Matsusaki M, Akashi M. Three-dimensional constructs induce high cellular activity: Structural stability and the specific production of proteins and cytokines. *Biochem Biophys Res Commun* 2010;402:153–157.
12. Decher G, Hong JD. Buildup of ultrathin multilayer films by a self-assembly process, 1. Consecutive adsorption of anionic and cationic bipolar amphiphiles on charged surfaces. *Macromol Chem Macromol Symp* 1991;46:321–327.
13. Decher G. Fuzzy nanoassemblies: Toward layered polymeric multicomposites. *Science* 1997;277:1232–1237.
14. Matsusaki M, Akashi M. Functional multilayered capsules for targeting and local drug delivery. *Expert Opin Drug Deliv* 2009;6:1207–1217.
15. Morita Y, Hata K, Nakanishi M, Nishisho T, Yura Y, Yoneda T. Cyclooxygenase-2 promotes tumor lymphangiogenesis and lymph node metastasis in oral squamous cell carcinoma. *Int J Oncol* 2012;41:885–892.
16. Morita Y, Hata K, Nakanishi M, Omata T, Morita N, Yura Y, Nishimura R, Yoneda T. Cellular fibronectin 1 promotes VEGF-C expression, lymphangiogenesis and lymph node metastasis associated with human oral and squamous cell carcinoma. *Clin Exp Metastasis* 2015;32:739–753.
17. Takeshita A, Iwai S, Morita M, Niki-Yonekawa A, Hamada M, Yura Y. Wnt5b promotes the cell motility essential for metastasis of oral squamous cell carcinoma through active Cdc42 and RhoA. *Int J Oncol* 2014;44:59–68.
18. Takahashi K, Kanazawa H, Akiyama Y, Tazaki S, Takahara M, Muto T, Tanzawa H, Sato K. Establishment and characterization of a cell line (SAS) from poorly differentiated human squamous cell carcinoma of the tongue. *J Jpn Stomatol Soc* 1989;38:20–28.
19. Momose F, Hirata S, Araida T, Tanaka N, Shioda S. Characters of three oral squamous cell carcinoma cell lines. *J Jpn Stomatol Soc* 1986;35:485–495.
20. Pittayapruek P, Meephanan J, Prapapan O, Komine M, Ohtsuki M. Role of matrix metalloproteinases in photoaging and photocarcinogenesis. *Int J Mol Sci* 2016;17:868.
21. Martin-Villar E, Borda-d'Agua B, Carrasco-Ramirez P, Renart J, Parsons M, Quintanilla M, Jones GE. Podoplanin mediates ECM degradation by squamous carcinoma cells through control of invadopodia stability. *Oncogene* 2015;34:4531–4544.
22. Steeg PS. Tumor metastasis: Mechanistic insights and clinical challenges. *Nat Med* 2006;12:895–904.
23. Joyce JA, Pollard JW. Microenvironmental regulation of metastasis. *Nat Rev Cancer* 2009;9:239–252.
24. Weis SM, Cheresh DA. Tumor angiogenesis: Molecular pathways and therapeutic targets. *Nat Med* 2011;17:1359–1370.
25. Friedrich J, Seidel C, Ebner R, Kunz-Schughart LA. Spheroid-based drug screen: Consideration and practical approach. *Nat Protoc* 2009;4:309–324.
26. Rodenhizer D, Gaude E, Cojocari D, Mahadevan R, Frezza C, Wouters BG, McGuigan AP. A three-dimensional engineered tumor for spatial snapshot analysis of cell metabolism and phenotype in hypoxic gradients. *Nat Mater* 2016;15:227–234.
27. Kenny PA, Lee GY, Myers CA, Neve RM, Semeiks JR, Spellman PT, Lorenz K, Lee EH, MH, Barcellos-Hoff MH, Peterson OW, Gray JW. The morphologies of breast cancer cell lines in three-dimensional assays correlate with these profiles of gene expression. *Mol Oncol* 2007;1:84–96.
28. Noma K, Smalley KSM, Lioni M, Naomoto Y, Tanaka N, El-Deiry W, King AJ, Nakagawa H, Herlyn M. The essential role of fibroblasts in esophageal squamous cell carcinoma-induced angiogenesis. *Gastroenterology* 2008;134:1981–1993.
29. Egeblad M, Werb Z. New functions for the matrix metalloproteinases in cancer progression. *Nat Rev Cancer* 2002;2:161–174.
30. Benson JD, Chen YN, Cornel-Kennon SA, Dorsch M, Kim S, Leszczyniecka M, Sellers WR, Lengauer C. Validating cancer drug targets. *Nature* 2006;441:451–456.